In Situ Surface Extended X-ray Absorption Fine Structure Spectroscopy of a Lead Monolayer at a Silver(111) Electrode/Electrolyte Interface

Mahesh G. Samant,[†] Gary L. Borges,[†] Joseph G. Gordon II,[†] Owen R. Melroy,*[†] and Lesser Blum[‡]

Contribution from IBM Almaden Research Center, K34/802, San Jose, California 95120, and the Physics Department, College of Natural Sciences, Rio Piedras, Puerto Rico 00931.
Received September 10, 1986

Abstract: With use of fluorescence detection and grazing incidence excitation, the X-ray absorption spectrum was obtained, at the PbL_{III} edge, of a monoatomic adlayer of lead on a silver(111) electrode immersed in solution. The adlayer was produced by underpotential deposition from aqueous lead acetate/sodium acetate electrolyte. The edge position and the near-edge structure confirm that the lead is fully reduced to the zerovalent state. The extended X-ray absorption fine structure (EXAFS) contains no detectable contribution from lead–silver scattering, either because the lead layer is incommensurate with the underlying silver lattice or because there is large thermal motion of the lead atoms. Instead, the fine structure is due to scattering from a single type of light atom, most likely oxygen. This oxygen must arise from adsorbed water molecules or acetate ions. The lead–oxygen distance changes with the electrode potential from 2.33 ± 0.02 Å at −0.53 V to 2.38 ± 0.02 Å at −1 V (vs. Ag/AgCl, 3 M KCl).

The structure of the metal/electrolyte interface and that of atoms or molecules adsorbed at this interface are long-standing questions of fundamental importance in electrochemistry. Yet there has been a lack of in situ studies on the atomic structure of wet electrodes because the presence of electrolyte makes it impossible to use the ultrahigh vacuum (UHV) techniques which are commonly used in surface science studies. These techniques are based on the scattering of electrons or ions, and their propagation distances in a condensed phase, such as an electrolyte, are too short. Still, these UHV techniques have provided significant insight into the nature of the absorbed species,[1] although the question of possible changes occurring during transfer of the electrode from the electrolyte to the vacuum remains unanswered. So far, successful in situ studies have relied primarily on ultraviolet, visible, or infrared radiation since their propagation distances in many solutions are suitably long. Such methods as surface enhanced Raman spectroscopy,[2] surface infrared spectroscopy,[3] surface plasmon spectroscopy,[4] and others have provided valuable information on the type and possible orientation of interfacial species. The techniques, however, only indirectly indicate geometrical structure. X-rays (of sufficiently high energy) have long propagation lengths in condensed matter and by measurement of diffraction and extended X-ray absorption fine structure spectroscopy (EXAFS)[5] can directly give geometrical information. Surface EXAFS (SEXAFS) seems particularly suitable for interfacial studies because it is sensitive to the local geometry and does not require long-range order. The major impediments to its use for surface studies have been the need for an intense X-ray source and the question of how to achieve surface selectivity. The advent of synchrotron X-ray sources now provides the high fluxes required, and we achieve surface selectivity by detecting the characteristic X-ray fluorescence of an atom which is unique in the interface.

Recent work has demonstrated that SEXAFS can provide structural information about monolayers of adsorbed atoms or molecules on metal[6] and semiconductor[7] surfaces. These measurements were performed in UHV with Auger or total electron yield techniques which, of course, are unsuitable for solutions. X-ray fluorescence yield measurements, however, offer the possibility of acquiring EXAFS from a surface buried in a condensed phase because of the large escape depth of the X-ray photons. It has already been established that EXAFS spectra can be obtained in fluorescence from samples where the absorbing element is present in minute quantities,[8] even monolayers.[9] The major problem in fluorescence detection is interference from the elastically and inelastically (Compton) scattered exciting beam. We have overcome this problem by using energy selective detection coupled with grazing incidence excitation, which simultaneously increases the X-ray intensity at the interface and drastically reduces the substrate scattering.[10] This paper describes the successful extension of SEXAFS to an electrochemical system.

The system studied was underpotentially deposited (UPD) lead on a silver(111) electrode. Silver is a well-characterized electrode material with a wide double layer region (potential range where no electrochemical reactions, such as metal dissolution or oxide formation, occur),[11] and it has been extensively used for studies of adsorption, electrode kinetics, and interfacial structure by a variety of techniques[12]. Lead has an L_{III} absorption edge at an accessible energy and its deposition on silver is well-behaved and occurs in discrete stages. The first monolayer is deposited at a potential that is less negative, by several hundred mV, than the thermodynamic deposition potential.[13] The initial deposition

* Author to whom inquiries should be addressed.
[†] IBM Almaden Research Center.
[‡] College of Natural Sciences.

(1) Hubbard, A. *Acc. Chem. Res.* **1980**, *13*, 177–184. Ross, P. N. *Surf. Sci.* **1981**, *102*, 463–485.
(2) Weaver, M. J.; Barz, F.; Gordon, J. G., II; Philpott, M. R. *Surf. Sci.* **1983**, *125*, 409–428.
(3) Pons, S. *J. Electroanal. Chem.* **1983**, *150*, 495–504. Bewick, J. *J. Electroanal. Chem.* **1983**, *150*, 481–493.
(4) Gordon, J. G., II; Ernst, S. *Surf. Sci.* **1980**, *101*, 499–506.
(5) Eisenberger, P.; Kincaid, B. M. *Science* **1978**, *200*, 1441–1447.
(6) Citrin, P. H.; Eisenberger, P.; Hewitt, R. C. *Phys. Rev. Lett.* **1978**, *41*, 309–312. Citrin, P. H.; Eisenberger, P.; Hewitt, R. C. *Surf. Sci.* **1979**, *89*, 28–40. Citrin, P. H.; Eisenberger, P.; Hewitt, R. C. *Phys. Rev. Lett.* **1980**, *45*, 1948–1951.
(7) Citrin, P. H.; Eisenberger, P.; Rowe, J. E. *Phys. Rev. Lett.* **1982**, *48*, 802–805. Citrin, P. H.; Rowe, J. E. *Surf. Sci.* **1983**, *132*, 205–211.
(8) Jaklevic, J.; Kirby, J. A.; Klein, M. P.; Robertson, A. S.; Brown, A. S.; Eisenberger, P. *Solid State Commun.* **1977**, *23*, 679–682. Hasting, J. B.; Eisenberger, P.; Lengler, B.; Perlman, M. L. *Phys. Rev. Lett.* **1979**, *43*, 1807–1810.
(9) Larison, B.; Rhodin, T. N.; Ho, W. *Solid State Commun.* **1985**, *55*, 925.
(10) Heald, S. M.; Keller, E.; Stern, E. A. *Phys. Lett.* **1984**, *103A*, 155–158.
(11) Valette, G.; Hamelin, A.; Parsons, R. *Z. Phys. Chem. (Frankfurt/Main)* **1978**, *113*, 71–89. Larkin, D.; Guyer, K. L.; Hupp, J. T.; Weaver, M. J. *J. Electroanal. Chem.* **1982**, *138*, 401–423. Bewick, A.; Thomas, B. *J. Electroanal. Chem.* **1977**, *84*, 127–140.
(12) Proceedings of the International Conference on Non-Tradiational Approaches to the Study of the Solid Electrolyte Interface: Furtak, T. E.; Kliewar, K. L.; Lynch, D. W., Eds. *Surf. Sci.* **1980**, *101*.
(13) Fleischman, R.; Robinson, J.; Waser, R. *J. Electroanal. Chem.* **1981**, *117*, 257–266.

0002-7863/87/1509-5970$01.50/0

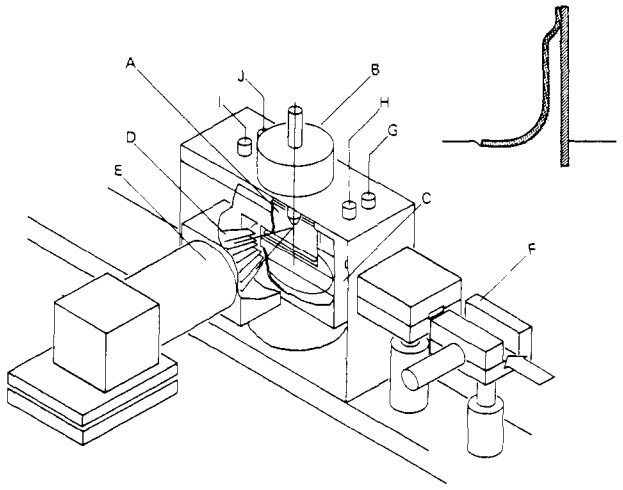

Figure 1. The schematic of the in situ electrochemical cell: (A) Lexan sample holder; (B) rotating stage; (C) Lexan cell; (D) Sollar slits; (E) high-purity germanium solid state detector; (F) slits; (G) port for reference electrode; (H) port for helium; (I) counter electrode; (J) port for electrolyte introduction. Inset: The electrode in thin film configuration.

occurs over a narrow range. The coverage changes from zero to saturation, approximately one hexagonal close-packed monolayer, and then remains constant for several hundred mV until the potential for bulk lead deposition is reached. By potentially clamping the electrode at a potential between that for the formation of the UPD layer and bulk deposition, a stable surface coverage of lead can be maintained for the duration of the experiment.

Experimental Section

Silver(111) electrodes were prepared by epitaxially depositing 2500 Å of Ag onto cleaved (in air) mica (ASTM V-2) surfaces which were maintained at 573 K during the deposition.[14] Epitaxy was confirmed by Laue x-ray diffraction backscattering. Scanning electron microscopy (SEM) pictures indicated that the Ag film was smooth (no steps or defects larger than 100 Å). In addition, the underpotential deposition of lead on these film electrodes was identical with that on bulk silver(111) single crystals. The films were stored in an inert atmosphere prior to use in the electrochemical cell.

A schematic of the electrochemical cell used is shown in Figure 1. The silver film on mica (A) was mounted on a Lexan holder which also contained the electrical contact. This Lexan (General Electric Co.) holder was attached to a rotating stage (B) that permitted alignment of the sample with respect to the beam. The elecrolyte was contained in a Lexan (General Electric Co.) cell (C) that was equipped with mylar windows in the X-ray beam path. The reference electrode (Ag/AgCl, 3M KCl) was introduced in cell through port (G). All potentials are reported with respect to this reference electrode. The cell was continuously purged with helium through tube H. The counter electrode (I) was a platinum wire and electrolyte was introduced into and removed from the cell through Teflon tube J. During data collection, the electrolyte level was lowered so that it was below the X-ray beam but above the bottom of the silver film. A thin layer of electrolyte was maintained by capillary action between the electrode surface and a 6.35 μm thick maylar film attached at the top of the electrode (see inset in Figure 1.) When the electrolyte level was raised, this film floated on the surface exposing the electrode to the bulk electrolyte.

The absorption spectrum was measured about the Pb L_{III} edge, at 13 040.6 eV, by monitoring the the Pb L_α fluorescence line at 10 550 eV. This was isolated by a 36 mm diameter high purity germanium solid state detector (E) (Ortec GLP-36360/13-S). Because of the nature of this detector it was necessary to limit the total intensity of X-rays impinging on it. Two things were done. First, the X-ray beam was incident on the sample at grazing incidence, i.e., angle of incidence greater than 89°, though the actual angle was not measured. This enhances the signal from the surfaces as the incident X-ray beam undergoes total external reflection,[10] increasing the intensity of X-rays at the surface at least by a factor of 2. Furthermore, since the penetration depth of X-rays in the sample is small, the scattered radiation is greatly reduced. The angle of

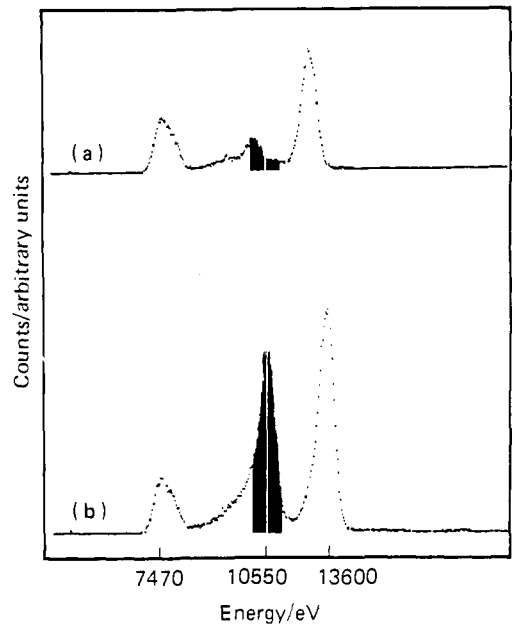

Figure 2. The energy resolved signal from the high purity germanium solid state detector: (a) incident energy 12 800 eV, pre-edge region; (b) incident energy 13 600 eV, post-edge region.

the sample was adjusted experimentally to minimize scattering while maximizing the fluorescence peak. Second, a germanium filter (approximately 40 μm thick) was used to preferentially absorb the elastic and Compton scattered radiation. Germanium has its K edge at 11 103.6 eV and thus has a substantially lower absorptivity for the Pb fluorescence at 10 550 eV than for the elastic and Compton scattering which lie at energies higher than 12 000 eV. Soller slits (D) were used to reduce the filter fluorescence incident on the detector. Slits (F) collimated the incoming beam and its intensity was measured by an ionization chamber. Figure 2, a and b, shows the energy-resolved fluorescence from the UPD Pb on Ag(111) sample with the incident energy respectively below and above the Pb absorption edge. The shaded region is the Pb fluorescence line. The detector resolution was approximately 650 eV, which was not fully adequate to separate the Ge and Pb fluorescence. The resolution was compromised to maintain a high detector count rate.

Data were collected in scans of 20 to 30 min, and many scans under a particular set of conditions were averaged to obtain higher signal-to-noise ratio. These data were analyzed by well-established procedures.[15] The major inflection point in the edge jump was taken to be the position of the edge. Bond distances were obtained by fitting the oscillatory part of the EXAFS equation[15] to the experimental oscillations with the phase shift for the pair of interest being obtained experimentally from reference compounds.

The electrolyte used was 0.5 M sodium acetate and 0.1 M acetic acid containing 5×10^{-5} M lead acetate, and it was prepared from Aldrich Gold label reagents in deionized water (Banrstead Nanopure). During electrodeposition, the level of the electrolyte was raised so that the entire surface of the electrode in the beam path was exposed to the bulk electrolyte. As a result of the low concentration of lead in solution, 10 min were required to form a monolayer at −0.53 V. The total charge transferred during the deposition step (measured by stripping the lead off) was 170 μC per cm^2 which correspnds to deposition of 5×10^{14} Pb atoms per cm^2. This is lower than the saturation coverage reported in the literature (300 μC per cm^2),[16] but the geometry of the cell makes it difficult to estimate the area exposed to the electrolyte and, in addition, the UPD process is well-known to be extremely sensitive to trace impurities. After the UPD layer was deposited, the electrolyte level was lowered until the lower end of the electrode was just immersed in the electrolyte. As previously indicated, a thin layer of electrolyte was held between the mylar film and the electrode surface by capillary action. The amount of lead held in the thin layer of solution (estimated to be less than 100 μm thick), based on its concentration in the bulk electrolyte, is less than 10% of a monolayer. Thus most of the lead fluorescence must come from the UPD surface layer. Furthermore, the diffusion of lead from

(14) Pashley, D. W. *Philos. Mag.* **1959**, *4* 316–323. Grunbaum, E. *Vacuum* **1973**, *24*, 153–164.

(15) Lee, P. A.; Citrin, P. A.; Eisenberger, P.; Kincaid, B. M. *Rev. Mod. Phys.* **1981**, *53*, 769–806.

(16) Takayanagi, K.; Kolb, D.; Kambe, K.; Lehmpfuhl, G. *Surf. Sci.* **1980**, *100*, 407–422.

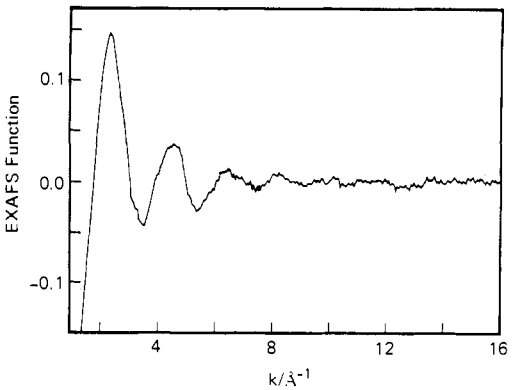

Figure 3. The EXAFS function for UPD Pb on Ag(111) film with the potential controlled at −0.53 V.

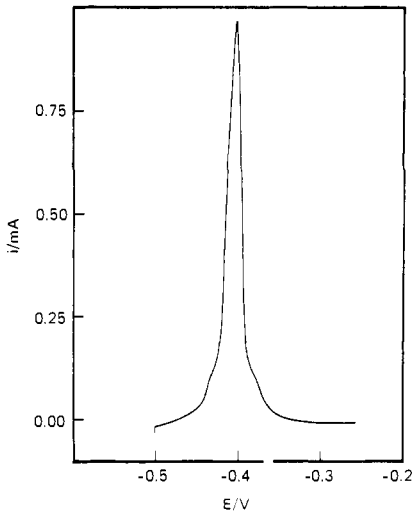

Figure 4. The voltamogram for stripping of Pb from the Ag(111) electrode at the end of the data collection.

the bulk electrolyte into this film was very slow and even permitted polarization of the electrode in the bulk deposition region without further significant lead deposition.

Results and Discussion

The structure of the UPD Pb layer was studied at two potentials, −0.53 and −1 V. At −0.53 V, which is between the underpotential and thermodynamic deposition potentials, the UPD layer is fully formed while no multilayer deposition occurs. At potentials positive of this by 0.1 V, there is no lead deposition and no lead fluorescence signal can be seen after the electrolyte is lowered, demonstrating that the amount of Pb contained in the thin solution layer is negligible.

Figure 3 shows the EXAFS function, $\chi(k)$ where k is photoelectron wave vector,[15] obtained from the UPD Pb on Ag(111) film potentiostated at −0.53 V. That the integrity of the electrode surface was maintained throughout the experiment can be seen from the voltammogram for the stripping of lead from the electrode obtained at the end of the data collection (Figure 4). This curve is identical with that obtained for a freshly deposited UPD layer. As will be discussed in the following section, the X-ray fluorescence signal can be unambiguously assigned to the reduced UPD Pb layer (as opposed to an oxidized solution species).

X-ray Absorption Edge Results. The X-ray absorption spectra of lead(II) acetate solution and the UPD Pb monolayer (at −0.53 V) are compared in Figure 5a, and spectra for Pb foil and lead acetate are compared in Figure 5b. The absorption edge of UPD Pb is at 13040.6 eV, which is the same as for Pb foil. The absorption edge energy for lead acetate is at 13041.8 eV, a shift of 1.2 eV to higher energy. This shift is expected because of the increase in the oxidation state of lead from 0 in the UPD layer to +2 in acetate solution. Figure 6 compares the absorption edges of the UPD Pb and PbO_2. The absorption edge of PbO_2 lies at

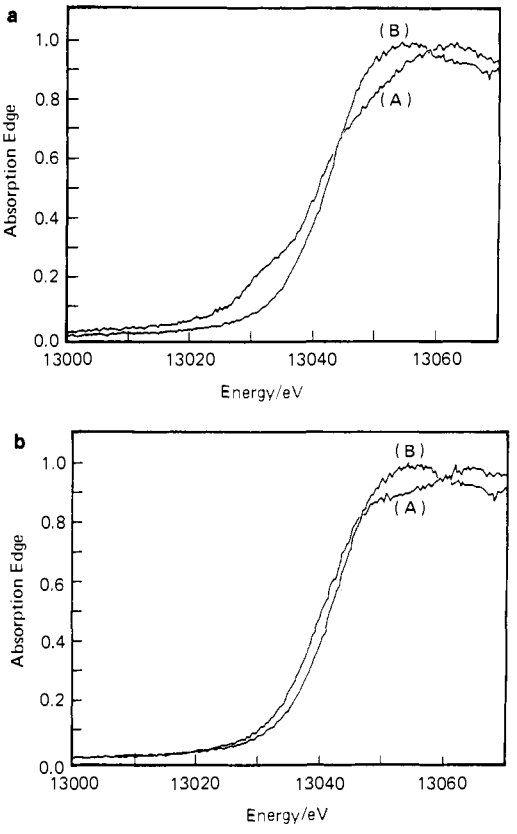

Figure 5. X-ray absorption spectra around the Pb L_{III} edge: (a) (A) UPD Pb on Ag(111), (B) lead acetate solution; (b) (A) Pb foil, (B) lead acetate solution.

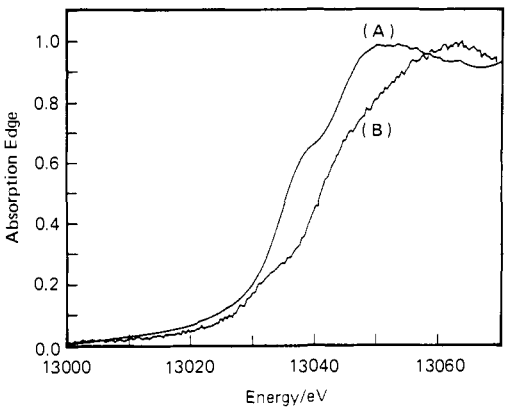

Figure 6. X-ray absorption spectra around the Pb L_{III} edge: (A) PbO_2; (B) UPD Pb on Ag(111) film.

13042.8 eV, 2.2 eV higher than the absorption edge of the UPD Pb or the Pb foil and 1.0 eV higher than the absorption edge in Pb acetate. This indicates that indeed the Pb whose fluorescence we are observing is completely reduced, which strongly suggests that it is deposited on the surface of the film and is not in solution. Figure 5a also shows a hump at the inception of the absorption edge jump for the UPD Pb, which is not present in the spectra of lead acetate or Pb foil. Furthermore, the UPD Pb does not show the resonance peak (at 13.055 keV) seen in lead acetate. These observations are further evidence that the UPD Pb is different form both bulk lead and aqueous Pb^{2+}. The fact that there is no indication of aqueous Pb^{2+} in the UPD lead spectrum confirms the earlier assertion that the amount of lead acetate in the thin liquid film on the electrode is negligible. It further indicates that the electrode is in fact under potential control as one would otherwise expect the UPD layer to have reoxidized. The PbO_2 also shows a hump in the pre-edge region similar to, but larger than, that of the UPD Pb. We suggest that this hump is associated with coordination to oxygen. It exists for PbO_2 and

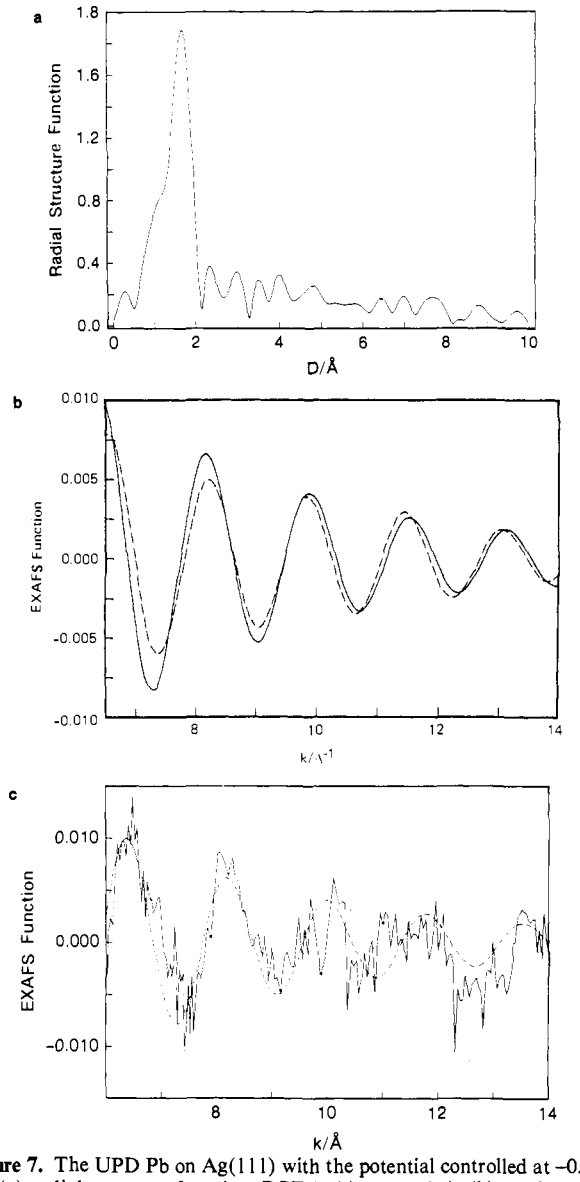

Figure 7. The UPD Pb on Ag(111) with the potential controlled at −0.53 V: (a) radial structure function, RSF (arbitrary units); (b) solid curve, the inverse Fourier transform of the major peak above, dashed curve, calculated EXAFS function for Pb–O distance of 2.33 Å; (c) comparison of the calculated and experimental EXAFS function.

UPD Pb, but not for lead foil or lead acetate. One possible explanation for the absence of this hump in lead acetate is that the water molecules coordinated to lead in aqueous Pb^{2+} are highly fluxional (i.e., the bonds are not rigid) and smear out the fine structure.

EXAFS Results. The Fourier transform of the product $\mathbf{k}^2\chi(\mathbf{k})$ for UPD Pb at −0.53 V, as shown in Figure 3, gives the radial Structure Function (RSF) shown in Figure 7a. The major peak in this RSF, located at 1.76 Å, is too short for a lead–silver distance. We propose that it corresponds to a lead–oxygen distance. No distinguishable peak appears at distances above 2 Å, which is where a peak corresponding to Pb–Ag scattering is expected. In constrast, the transform of the EXAFS from an alloy consisting of 1% by weight of Pb in Ag has a prominent peak corresponding to Pb–Ag scattering at 2.64 Å, as can be seen in Figure 8b. Figure 8a shows $\chi(\mathbf{k})$ for the Pb–Ag alloy and Figure 8b, the Fourier transform of the product $\mathbf{k}^2\chi(\mathbf{k})$. The lack of a peak in the UPD spectrum corresponding to Pb–Ag scattering can be explained by a large Debye–Waller factor (the Debye–Waller factor in the EXAFS expression is not the same as the Debye–Waller factor in X-ray diffraction and does not have the same quantitative significance[15]) for the lead in the adlayer or by its being incommensurate with silver surface or both. The

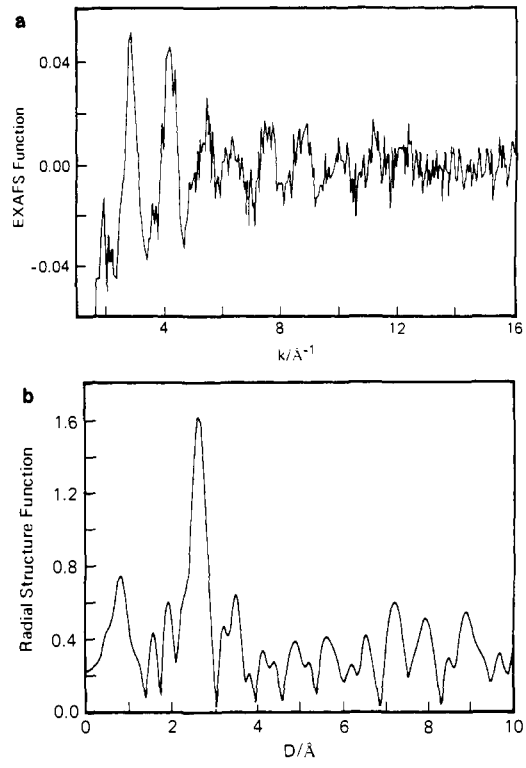

Figure 8. Pb–Ag alloy: (a) the EXAFS function; (b) radial structure function, RSF (arbitrary units).

absorption spectrum of polycrystalline lead foil collected during this study did not show any fine structure. This is probably a manifestation of a large Debye–Waller factor for Pb, a direct result of its low melting point (600 K). The melting temperatures of Pb monolayers on Cu single crystals are reported to be lower than the bulk value and are dependent on the crystal face[17]. It is reasonable to expect that the melting point of a Pb monolayer on Ag would also be lower than the bulk value. This should lead to a sufficiently large Debye–Waller factor that no Pb–Ag structure would be seen in the EXAFS. Furthermore, the UPD Pb almost certainly forms an incommensurate structure atop Ag(111) due to the significant difference in atomic radii between Pb and Ag (1.75 and 1.44 Å, respectively). Indeed, the saturation coverage, evaluated from the total charge transferred, is consistent with a hexagonal close-packed monolayer of Pb with normal Pb–Pb spacing[16]. An incommensurate structure would have multiple Pb–Ag distances each of which would give rise to oscillations of different periods and thus would damp the overall EXAFS oscillations arising from Pb–Ag distances. The efects of an incommensurate structure and a large Debye–Waller factor are similar, and it is not possible to distinguish the two from the EXAFS data alone.

It should be pointed out that the incident X-ray beam was polarized with its **E** vector perpendicular to the surface of the sample. Since structural information can only be obtained from atom–atom vectors which have a non-zero projection on the **E** vector,[18] no information on lead–lead distances, which lie in the surface and are hence perpendicular to the **E** vector, can be obtained from these spectra.

The main peak in the RSF shown in Figure 7a was inverse Fourier transformed to filter out noise and the result is shown in Figure 7b. In addition to the position of the peak in the RSF being incompatible with a Pb–Ag distance, the amplitude function of the inverse transform is compatible only with scattering from a first-row element. Given the composition of the solution, the most likely candidate is oxygen, and fitting the inverse Fourier transform to the EXAFS equation, using the Pb–O phase shift and amplitude

(17) Henrion, J.; Rhead, G. E. *Surf. Sci.* **1972**, *29*, 20–36.
(18) Stohr, J.; Jaeger, R.; Brennan, S. *Surf. Sci.* **1982**, *117*, 503–524.

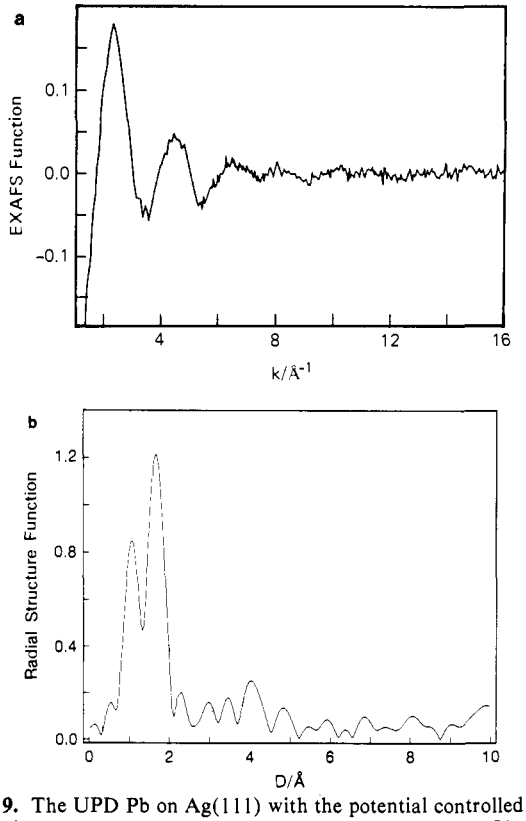

Figure 9. The UPD Pb on Ag(111) with the potential controlled at −1 V: (a) the EXAFS function; (b) radial structure function, RSF (arbitrary units).

functions obtained from the PbO_2 EXAFS, yields the fit shown in Figure 7b. For comparison, the calculated and experimental EXAFS equation are superimposed in Figure 7c (only the region above a **k** of 6 $Å^{-1}$ is considereed in the analysis to avoid complications from near-edge structure). The Pb–O distance was found to be 2.33 ± 0.02 Å. This is longer than the 2.16–2.22 Å in PbO_2 and 2.30 Å in red PbO[19] and is consistent with the lead being in a more reduced oxidation state. As both the absorption edge and the EXAFS indicate that the UPD layer is reduced, effectively eliminating oxide as the source of oxygen, one must conclude that the oxygen comes from chemisorbed water or acetate ions. These are indistinguishable by EXAFS.

The observation of strong wiggles from Pb–O scattering is surprising and clearly means that the distribution of Pb–O distances is small, much smaller, for example, than in aquated Pb^{2+} where the EXAFS wiggles are much more strongly damped. This may indicate that the adsorbed oxygen atoms are fairly rigidly attached and occupy specific sites. But it is more probably a manifestation of the layering of solvent molecules near a surface such as has been observed in the experiments of Isrealachvili[20] and in recent computer simulations.[21] An absorption spectrum was also obtained with the electrode polarized at −1 V and yielded the $\chi(\mathbf{k})$ shown in Figure 9a and the Fourier transform (of the product $\mathbf{k}^2\chi(\mathbf{k})$) shown in Figure 9b. Since −1 V is far negative of the reversible lead potential, special care must be taken to avoid bulk lead deposition. To accomplish this, the potential of −1 V was applied only after the solution level was lowered following complete deposition of the UPD Pb layer. It is important to note that hydrogen evolution does not occur on lead (at this pH) at this potential. The spectra closely resemble the corresponding curves for −0.53 V with a single major peak in the region where Pb–O should be and no peak corresponding to a Pb–Ag distance. The smaller peak on the shoulder of the Pb–O peak is primarily a result of poorer signal to noise in the raw EXAFS. Because of time restrictions, only half as many scans were acquired at this potential. As can be seen from a comparison of the filtered EXAFS spectra for the two potentials, shown in Figure 10, there is a clear difference between the data taken at −0.53 and at −1 V. Applying the same analysis procedure as above yields a Pb–O distance of 2.38 ± 0.02 Å at −1 V. This distance is 0.05 Å longer than that obtained with the electrode at −0.53 V, which is consistent with the negatively charged electrode repelling a negatively charged or strongly dipolar adsorbate. If water is indeed the adsorbate, then this behavior, coupled with the short Pb–O distance, implies that even at this negative potential, the water is adsorbed with the oxygen end toward the electrode.

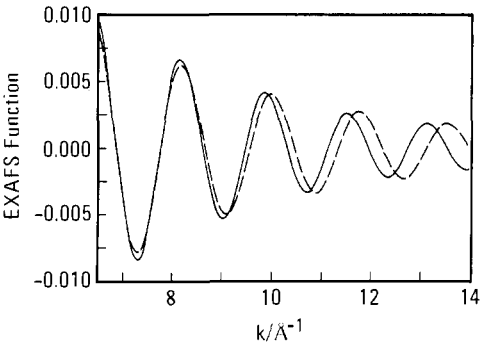

Figure 10. Inverse Fourier transforms of the RSFs: solid curve, −1 V; dashed curve, −0.53 V.

Conclusions

This experiment demonstrates that it is possible to obtain useable SEXAFS spectra of monolayers on electrodes despite the presence of a condensed phase and, further, that the absorption spectra can provide valuable information about the composition and structure of the interface. In the present case, they clearly show that the lead atoms in the adlayer are completely reduced and that either they lie on a lattice that is incommensurate with the underlying Ag(111) surface or are very mobile at room temperature (or both). The observed scattering from a light atom, the most likely candidate for which is oxygen, implies that water or acetate ions are chemisorbed on the UPD Pb layer. The Pb–O distance varies from 2.33 ± 0.02 Å at an electrode potential of −0.53 V to 2.38 ± 0.02 at −1 V. This behavior is consistent with a low oxidation state for lead and a negatively charged or a dipolar adsorbate with the negative end toward the surface.

Acknowledgment. This work was partially supported by the Office of Naval Research and was carried out at the Stanford Synchrotron Radiation Laboratory (SSRL), which is supported by the Department of Energy.

Registry No. Pb, 7439-92-1; Ag, 7440-22-4.

(19) Wyckoff, R. W. G. *Crystal Structures*, 2nd ed.; J. Wiley and Sons: New York, 1963.
(20) Isrealachvili, J. N. *Chem. Sci.* **1985**, *25*, 7–14.
(21) Henderson, D.; Blum, L.; Lozada-Cassou, M. *J. Electroanal. Chem.* **1983**, *150*, 291–303.